

Simultaneous Calibration of a Structured light-based Catadioptric Stereo Sensor

Dieu Sang Ly and El Mustapha Mouaddib
Laboratoire MIS
Equipe Perception-Robotique
Université de Picardie Jules Verne, Amiens, France
lydieusang@yahoo.com and mustapha.mouaddib@u-picardie.fr

Joaquim Salvi
Computer Vision and Robotics Group
Institute of Informatics and Applications
Universitat de Girona, Spain
J.Salvi@hw.ac.uk

Abstract—Omnidirectional vision systems enlarge the field of view of conventional cameras by means of special lenses, multi-image acquisition systems or catadioptric cameras. Catadioptric cameras are the customary ones coupled with mirrors of special curvatures to obtain an entire field of view. Structured light projection is widely used to solve the correspondence problem in stereo computation. A structured light-based catadioptric stereo sensor is formed by a catadioptric camera and an omnidirectional laser projector. In the most recent work on catadioptric stereo system based on structured light projection, the catadioptric camera and the omnidirectional laser projector are calibrated sequentially to estimate the parameters of each component. This thesis proposes a novel approach which permits a simultaneous calibration for both of them. The proposed method simplifies the process of sequential calibration while preserving the accuracy of the scene reconstruction. Particularly the simultaneous approach provides an important improvement when it does not require an accurate measurement of the calibration patterns in 3D space as the sequential approach does.

Index Terms—Omnidirectional vision, stereo vision, structured light, calibration.

I. INTRODUCTION

Omnidirectional vision describes the perception of a vision system that can image the surroundings in all directions. There exist different devices that enlarge the field of view of conventional cameras, but most can be divided into three main groups: special lenses such as fish-eye lenses, multi-image acquisition systems and catadioptric cameras.

The original catadioptric sensor has been initially proposed by Rees in 1970. In the US patent [1], Rees proposed the use of a hyperboloidal mirror with a camera to capture catadioptric images which could be mapped to traditional perspective images. Twenty years later, Yagi and Kawato generated an omnidirectional camera using a conical mirror [2]. The sensor, namely COPIS (CONical Projection Image Sensor), was mounted on a mobile robot and used to capture the indoor scene. Afterwards, Hong and the others studied the catadioptric sensor with a spherical mirror [3]. In 1993, Yamazawa and his colleagues employed again a hyperboloidal mirror in their omnidirectional sensor [4]. The conical mirror was also applied in the SYCLOP (CONical SYstem for LOCALization and Perception) sensor by researchers at University of Picardie Jules Verne, led by Mouaddib [5]. In 1997, Nayar and Baker developed an ideal omnidirectional vision

sensor combining a paraboloidal mirror and a telecentric lens [7]. During the past decade, omnidirectional vision has been growing continuously as a great number of researches in computer vision have been dedicated to omnidirectional sensors. In [8], Baker and Nayar have derived a complete class of single-lens single-mirror sensors having a single viewpoint (SVP) with references to omnidirectional systems that have been proposed in literature.

Stereo technique is used to obtain the range information of the scene from its images captured by cameras at different points of observation. Nene and Nayar proposed the catadioptric sensors for stereo computation using a single camera pointing towards multiple mirrors instead of two cameras frequently used in conventional stereo systems [13]. Gluckman and others introduced in [14] the panoramic stereo system composed of two vertically aligned (coaxial) paracatadioptric sensors, each of which combines an orthographic camera with a parabolic mirror and hence verifies the single viewpoint constraint. Later, Ollis and others simulated different catadioptric stereo systems with two hyperbolic mirrors and one or two cameras [15].

The correspondence problem remains interesting in stereo vision. This problem can be simplified using structured light method in which the second stereo camera is replaced by a light projector. From the deformation of the imaged pattern compared to the projected one, the 3D information can be achieved. Among various types of structured light patterns which can be used in stereo vision system, laser seems to be a good choice as its monochromatic property permits optical filters to be used for image segmentation, such intense light like laser enhances the matching and laser projectors can be easily coupled in a compact device [17].

Orghidan and others have developed a stereo vision system using a catadioptric camera and applying structured light technique [19]. The proposed sensor has the coaxial configuration similar to the paracatadioptric stereo system created by Gluckman in [14] but the lower catadioptric sensor is replaced by an omnidirectional laser projector as illustrated in figure 1. In [19], the catadioptric camera and the laser projector have been calibrated consecutively. This paper proposes a novel method to calibrate these two components concurrently.

The sequential calibration already developed for this sensor is presented in section II. The novel calibration method,

namely simultaneous calibration, is detailed in section III. The experimental results are shown in section IV. The article is ended with the conclusions.



Fig. 1. Structured light-based catadioptric stereo sensor

II. SEQUENTIAL CALIBRATION

The sensor calibration is called sequential calibration as it consists of two stages: calibration of the catadioptric camera and afterwards that of the omnidirectional laser projector.

A. Catadioptric camera calibration

In [21], Geyer and Daniilidis have shown that every central catadioptric projection is equivalent to a central projection of the scene point to a sphere followed by a perspective projection from a point on the diameter of the sphere to a plan perpendicular to that diameter as shown in figure 2. Orghidan has used this projective equivalence to model and calibrate the catadioptric camera using parabolic mirror.

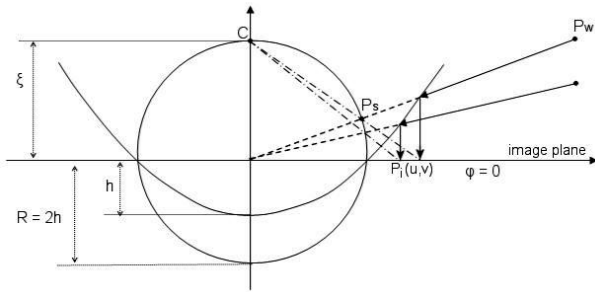


Fig. 2. The equivalence of a SVP catadioptric projection and a projection on a sphere

The unified model of the catadioptric camera is expressed in equation (1).

$$\begin{cases} u = \alpha_u \frac{(\xi + \varphi)x_W}{\xi \sqrt{x_W^2 + y_W^2 + z_W^2} - z_W} + u_0 \\ v = \alpha_v \frac{(\xi + \varphi)y_W}{\xi \sqrt{x_W^2 + y_W^2 + z_W^2} - z_W} + v_0 \end{cases} \quad (1)$$

The catadioptric camera is calibrated using a set of known 3D points $P_W(x_W, y_W, z_W)$ distributed on four calibration planes enclosing the sensor and the corresponding pixel points

(u, v) extracted in the omnidirectional image.

The calibration parameters are as follows:

- ξ depending on the eccentricity, φ depending on the eccentricity and the scale
- $\alpha_u, \alpha_v, u_0, v_0$: intrinsic camera parameters
- $\alpha, \beta, \gamma, t_X, t_Y, t_Z$: extrinsic camera parameters describing the orientation and translation of the camera with respect to the world

From the 3D points, the pixel points are calculated using the unified model. The distance between the computed pixels and those being detected in the captured image is minimized by a non-linear iterative algorithm such as Levenberg-Marquardt. The catadioptric camera parameters are estimated after the minimization.

B. Omnidirectional laser projector calibration

The omnidirectional laser projector is composed of a laser source that emits a laser circle to a conical mirror. If the laser emitter and the conical mirror are perfectly aligned, the laser reflected by the mirror spreads out the surroundings as a cone of optical rays as shown in figure 3a. These optical rays intersect with known calibration planes forming a set of 3D points which can be captured by the catadioptric camera. The locations of these 3D laser points can be computed from their 2D projections in the image and the camera parameters obtained from the catadioptric camera calibration. In other words, the 2D points are back-projected to the points on the sphere using camera parameters estimated in the previous stage. The intersections of the optical rays passing through those points on the sphere and the known calibration planes determine the 3D laser points. Then, a quadratic surface is fitted to these points to present a parameterised model of the laser projection.

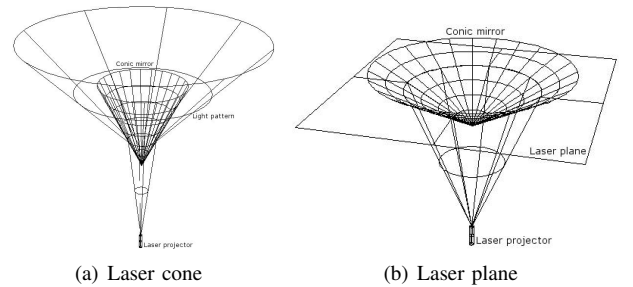


Fig. 3. Omnidirectional projection of a structured light

If there is a special configuration between the aperture angle of the conical mirror and the fan angle of the emitted laser cone, the projected pattern becomes a plane as illustrated in figure 3b. And in that case, the intersections of the laser and the calibration planes are straight lines which are imaged to elliptical arcs in the catadioptric image. The prototype used by Orghidan in [19] satisfies this particular configuration. Therefore, the laser projection is parameterised by a plane described in equation (2).

$$ax + by + cz + d = 0 \quad (2)$$

III. SIMULTANEOUS CALIBRATION

The simultaneous calibration requires a complete model that relates the 3D laser points and their image points through the parameters of the camera and the laser projection. This complete model is derived in the following sections.

Considering a laser point $P_W(x_W, y_W, z_W)$ with respect to the camera coordinate system $\{C : x_C, y_C, z_C\}$ centred at the focus of the parabolic mirror (or the centre of the sphere), its pixel coordinates (u, v) can be obtained from equation (1) using the catadioptric camera parameters $(\xi, \varphi, \alpha_u, \alpha_v, u_0, v_0)$.

Supposing that the laser emitter and the conical mirror are perfectly aligned, the 3D shape of the reflected laser pattern is a vertical circular cone. The apex of this cone is chosen as the origin of the laser coordinate system $\{L : x_L, y_L, z_L\}$ as illustrated in figure 4. To simplify the problem, let $\{L\}$ be the translation of $\{C\}$ along the Z-axis with a distance h , therefore the location of $\{L\}$ with respect to $\{C\}$ is $(0, 0, -h)^T$. And there is no rotation between $\{C\}$ and $\{L\}$. The baseline between the camera and the laser coordinate systems is vertical.

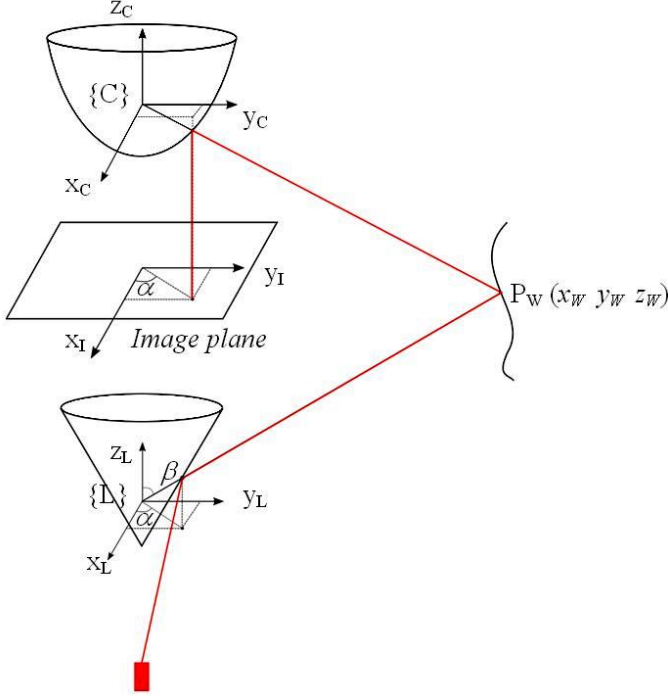


Fig. 4. Triangulation of the laser point in 3D space, the camera and the laser projection coordinate systems

The fact the laser point P_W also belongs to an optical ray in the cone of laser can be exploited to describe the connection of the 3D and 2D points through the parameters of the laser projection. The azimuth angle and the tilt angle of this ray in the laser coordinate system $\{L\}$ are α and β respectively as shown in figure 5. This optical beam can be expressed in $\{L\}$ by equation (3).

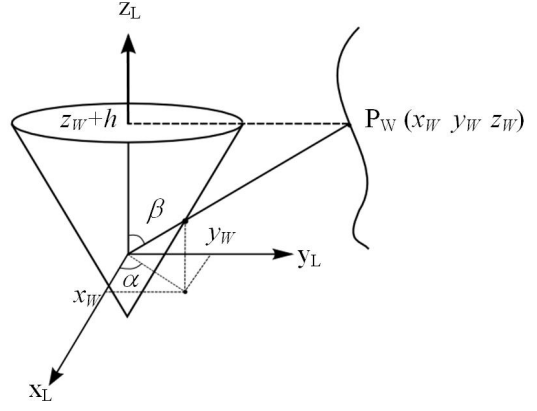


Fig. 5. Geometry of an optical ray in the cone of projected laser pattern

$$\begin{cases} x_W = (z_W + h) \cdot \tan\beta \cdot \cos\alpha \\ y_W = (z_W + h) \cdot \tan\beta \cdot \sin\alpha \end{cases} \quad (3)$$

In equations (3), h and β are the parameters representing the cone of laser projection. h represents the position of the laser-conical mirror set with respect to $\{C\}$. β depends on the fan angle of the laser emitted from the source and the open angle of the laser mirror (conical one). The azimuth angle α of any laser ray is also the angle between the vertical plane containing that ray and the vertical plane containing the X-axes of all coordinate systems. Therefore, the angle α can be computed in the image plane by equation (4).

$$\begin{cases} \cos\alpha = \frac{x_I}{\sqrt{x_I^2 + y_I^2}} \\ \sin\alpha = \frac{y_I}{\sqrt{x_I^2 + y_I^2}} \end{cases} \quad (4)$$

where (x_I, y_I) are can be calculated from the pixel coordinates as follows:

$$\begin{cases} x_I = \frac{u - u_0}{\alpha_u} \\ y_I = \frac{v - v_0}{\alpha_v} \end{cases} \quad (5)$$

From equations (3), (4) and (5), we obtain:

$$\begin{cases} x_W = (z_W + h) \cdot \tan\beta \cdot \left(\frac{u - u_0}{\alpha_u}\right) / \sqrt{\left(\frac{u - u_0}{\alpha_u}\right)^2 + \left(\frac{v - v_0}{\alpha_v}\right)^2} \\ y_W = (z_W + h) \cdot \tan\beta \cdot \left(\frac{v - v_0}{\alpha_v}\right) / \sqrt{\left(\frac{u - u_0}{\alpha_u}\right)^2 + \left(\frac{v - v_0}{\alpha_v}\right)^2} \end{cases} \quad (6)$$

The above equations relate the 3D laser points and the pixel points by the intrinsic parameters of the camera and the parameters of the laser projection.

Equations (1) and (6) are the complete model of the sensor which allows the parameters of the catadioptric camera $(\xi, \varphi, \alpha_u, \alpha_v, u_0, v_0)$ and the omnidirectional laser projection (h, β) to be solved from a set of 3D points (x_W, y_W, z_W) and 2D points (u, v) by a non-linear iterative algorithm such as Levenberg Marquardt.

An interesting remark is that there are four equations in (1) and (6) for each laser point in 3D space; hence 4N equations for N points. If the locations of these laser points

(x_W, y_W, z_W) are also unknowns, there are $3N+8$ unknowns. As the number of equations is superior to the number of unknowns, it is possible to estimate eight parameters defined above and the locations of 3D points from their image points with a sufficient number of equations. However, a system of non-linear equations may have different solutions, and in that case more constraints are necessary to obtain the correct solution.

IV. EXPERIMENTAL RESULTS

The sequential calibration derived in [19] and the simultaneous calibration proposed in this paper will be evaluated under simulation.

Firstly, the parameters of the sensor $(\xi, \varphi, \alpha_u, \alpha_v, u_0, v_0, h, \beta)$ are generated as follows:

- The mirror is parabolic: $\xi = 1$ and $\varphi = 0$
- The intrinsic parameters of the camera: $\alpha_u = 55, \alpha_v = -55, u_0 = 400$ and $v_0 = 300$
- The cone of laser projection: $h = 200$ and $\beta = \frac{\pi}{3}$

The synthetic 3D points represents the intersections of the cone of laser pattern and several walls placed around the sensor as shown in figure 6a. Then, the pixel points as demonstrated in figure 6b are computed from the 3D points and the parameters of the sensor using the camera model in equation (1).

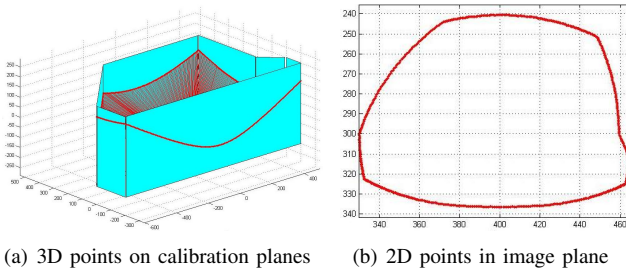


Fig. 6. Synthetic laser points

These set synthetic points are used for both calibration methods to evaluate and compare their performance. Each calibration method is evaluated by eight trials in which:

- Various Gaussian noises are added to the synthetic 3D points to simulate the error in the measurement of the 3D points.
- Various Gaussian noises are added to the computed pixel points to simulate the error in the pixel detection in images.
- Various sets of parameters are tested to verify the ability of convergence of the non-linear iterative approach.

Note that the same noises and sets of parameters are used for both methods in each trial to validate the comparison.

The calibration methods are also evaluated with a surrounding scene of two different ranges: small range with a dimension of about 1000mm and large range of 5000mm. The reconstruction errors of two approaches are illustrated

in figures 7 and 8. There are 580 laser points in total. The presented error is the average distance from the reconstructed 3D points and the synthetic ones generated at the beginning of the simulation.

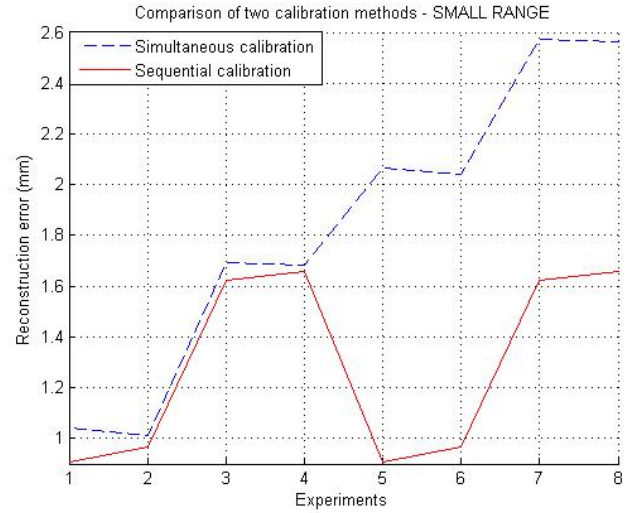


Fig. 7. Reconstruction errors of the sequential and simultaneous calibrations with a surrounding environment of small range

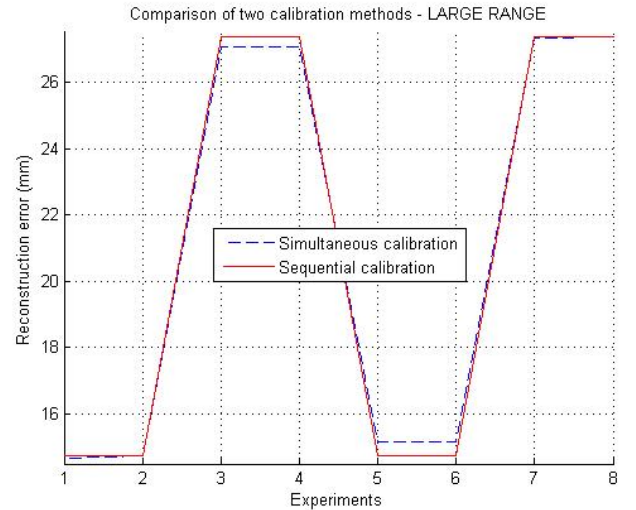


Fig. 8. Reconstruction errors of the sequential and simultaneous calibrations with a surrounding environment of large range

It can be seen that the novel calibration provides slightly higher reconstruction errors than the sequential calibration if the environment is small (from figure 7), but better results with a large environment (from figure 8). The possible reason is that the sequential calibration performs well with the calibration patterns enclosing the sensor at short distances. A better accuracy with the large environment should be an advantage of the simultaneous method over the other because this novel method allows the 3D points to be reconstructed along with the calibration as mentioned in section III and the reconstruction

is usually carried out with a large surrounding scene.

The complete model of the simultaneous calibration presented in equations (1) and (6) has shown that this method can also solve the parameters if the 3D points are not well defined as there are $(3N+8)$ unknowns (eight parameters and $3N$ coordinates of N points) and $4N$ equations. However, the non-linear system in (1) and (6) may have different solutions, and in that case using only the pixel points is not sufficient to estimate the sensor parameters and the unknown 3D points; hence some constraint about the 3D points is necessary. This constraint can be an estimation about the 3D laser points as presented in the next experiment.

The two calibrations are again evaluated using a special set of 3D points. This set of 3D points is not the one created at the beginning of the simulation but has the similar structure. This means that the 3D points are not measured but they are estimated when the laser is projected to the scene. For example, the scene is structured by seven walls as illustrated in figure 6a, the laser spots on these walls can be estimated as follows: x and y are estimated from the locations of these walls with respect to the sensor and z is estimated from x, y and the shape of the laser cone. In other words, the coordinates of the laser points projected to the scene can be approximated by the structure of the scene.

Figures 9 shows the comparison result of the sequential and simultaneous calibrations with the increased error in the approximation of the 3D points. It is obviously that the simultaneous method is much better than the sequential one if the 3D points used for calibration are not accurately measured. In an environment of about 5000 mm, using a set of 3D points with an approximation error of 5%, the reconstruction error of the simultaneous approach is about 90 mm (0.18% of the scene dimension) whereas the sequential one provides an error of about 310 mm (0.62% of the scene dimension). Moreover, the error created by the sequential method raises significantly when the uncertainty about the structure of the scene to be reconstructed increases.

V. CONCLUSION

This paper presented a novel calibration approach for the catadioptric stereo sensor based on structured light projection. It is proved by simulation to be simpler and more robust than the calibration that has been developed for the same stereo system. These two calibration methods are evaluated and compared by using the same set of synthetic 3D and 2D points. The experimental results have shown that:

- Two calibration methods provide similar reconstruction accuracy if the 3D points use for the calibration are well known.
- Concerning the sensor modelling, the sequential method uses the projection model of the camera while the simultaneous one adds to that model the representation of the laser projection. However, the laser projection is easily modelled by geometry; hence, there is no significant complexity.

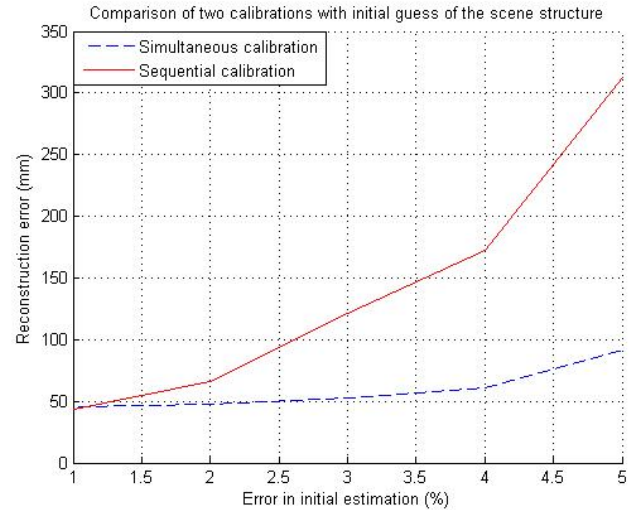


Fig. 9. Reconstruction errors of two calibrations using 3D points approximated from the scene structure with a surrounding environment of large range

- The sequential method requires the calibration patterns placed around the sensor whereas the simultaneous one does not as it can employ directly the laser profile projected to the scene. Moreover, in the sequential approach, the 3D points should be well measured to ensure a reliable calibration. This limitation is overcome by the simultaneous calibration in which the 3D laser points can be approximated from the structure of the scene.

The further step will be to validate this method with the prototype of the structured light-based catadioptric stereo sensor in the laboratory. Once the sensor is calibrated, it can be used for further applications such as scene reconstruction, environment inspection, robot navigation, etc. Therefore, an interesting research path is to embed this stereo sensor on a mobile robot to assist this automaton in the localisation, navigation and mapping tasks.

ACKNOWLEDGMENT

First of all, I would like to thank Mr. El Mustapha Mouadib, my Master thesis director, for offering me an opportunity to work in the MIS laboratory, one of the pioneers in the field of omnidirectional vision. During three months of the thesis, he has shared with me his experience, his passion for research. I did make much progress in my thesis due to his thorough instruction. Special thank to Mr. Joaquim Salvi, my second director, for leading me to this research field and for the helpful advice he has given me during my period of research. I would like to show my gratitude to the teaching staffs of Heriot Watt University, Universitat de Girona and Université de Bourgogne who have brought me much helpful knowledge as well as research experience during the Master. I should also mention my gratefulness to Pascal, Cédric, Guillaume and Ali at MIS laboratory.

REFERENCES

- [1] D.W. Rees. Panoramic television viewing system. In *United States Patent* No. 3, 505, 465, 1970.
- [2] Y. Yagi and S. Kawato. Panoramic scene analysis with conic projection. In *IEEE/RSJ International Conference on Intelligent Robots and Systems*, Vol. 1, pp. 181-187, 1990.
- [3] J. Hong, X. Tan, B. Pinette, R. Weiss and E.M. Riseman. Image-based homing. In *IEEE International Conference on Robotics and Automation*, pp. 620-625, vol. 1, 1991.
- [4] K. Yamazawa, Y. Yagi and M. Yachida. Omnidirectional imaging with hyperboloidal projection. In *IEEE/RSJ International Conference on Intelligent Robots and Systems*, pp. 1029-1034, 1993.
- [5] C. Pegard and E.M. Mouaddib. A mobile robot using a panoramic view. In *IEEE International Conference on Robotics and Automation*, Vol. 1, pp. 89-94, 1996.
- [6] S.K. Nayar. Catadioptric omnidirectional camera. In *IEEE International Conference on Computer Vision and Pattern Recognition*, pp. 482-488, 1997.
- [7] S.K. Nayar and S. Baker. Catadioptric image formation. In *Proceedings of DARPA Image Understanding Workshop*, pp. 1431-1437, 1997.
- [8] S. Baker and S.K. Nayar. A Theory of Single-Viewpoint Catadioptric Image Formation. In *International Journal of Computer Vision* 35(2), 175-196, 1999.
- [9] V.S. Nalwa. A true omnidirectional viewer. In Technical report, Bell Laboratories, Holmdel, NJ 07733, USA, February 1996.
- [10] Y. Yagi and M. Yachida. Real-time generation of environmental map and obstacle avoidance using omnidirectional image sensor with conic mirror. In *Proceedings of the 1991 Conference on Computer Vision and Pattern Recognition*, pp. 160-165, June 1991.
- [11] S. Bogner. Introduction to panoramic imaging. In *Proceedings of the IEEE SMC Conference*, pp. 3100-3106, October 1995.
- [12] J.R. Murphy. Application of panoramic imaging to a teleoperated lunar rover. In *Proceedings of the IEEE SMC Conference*, October 1995.
- [13] S.A. Nene and S.K. Nayar. Stereo with mirrors. In *Sixth International Conference on Computer Vision*, pp. 1087-1094, 1998.
- [14] J. Gluckman, S.K. Nayar and K.J. Thoresz. Real-Time omnidirectional and Panoramic Stereo. In *Proceedings of the 1998 DARPA Image Understanding Workshop*, Monterey, California, 1998.
- [15] M. Ollis, H. Herman and S. Singh. Analysis and Design of Panoramic Stereo Vision Using Equi-Angular Pixel Cameras. In Technical report CMU-RI-TR-99-04, Robotics Institute, Carnegie Mellon University, January 1999.
- [16] J. Battle, E.M. Mouaddib and J. Salvi. A Survey: Recent Progress in Coded Structured Light as a Technique to Solve the Correspondence Problem. In *Pattern Recognition* 31(7), pp. 963-982, July 1998.
- [17] R. Orghidan, J. Salvi and E.M. Mouaddib. Calibration of a structured light-based stereo catadioptric sensor. In *Workshop on Omnidirectional Vision, IEEE International Conference on Computer Vision and Pattern Recognition*, 2003.
- [18] R. Orghidan, E.M. Mouaddib and J. Salvi. Omnidirectional depth computation from a single image. In *IEEE International Conference on Robotics and Automation*, pp. 1234-1239, 2005.
- [19] R. Orghidan. Catadioptric stereo based on structured light projections. PhD thesis, Universitat de Girona, 2006.
- [20] C. Mei. Laser-augmented omnidirectional vision for 3D localisation and mapping. PhD thesis at Ecole Nationale Suprieure Des Mines De Paris Sophia Antipolis, 2007.
- [21] C. Geyer and K. Daniilidis. Equivalence of catadioptric projections and mappings of the sphere. In *First Workshop of Omnidirectional Vision*, pp. 91-96, 2000.
- [22] Y. Yagi. Omnidirectional sensing and its applications. In *IEICE Transactions on Information and Systems*, Vol. E82-D, pp. 568-578, 1999.
- [23] S.S. Lin and R. Bajcsy. The true single view point (SVP) configuration for omni-directional view catadioptric system using cone mirror. In Technical report MS-CIS-00-24. Computer and Information Science Department, University of Pennsylvania, Philadelphia, USA, 2001.
- [24] T. Svoboda and T. Pajdla. Epipolar Geometry for central catadioptric cameras. In *International Journal of Computer Vision* 49(1), pp. 23-37, 2002.